

The Usefulness of Seismic Attribute Mapping in the Interpretation of Submarine Channel Seismic Geomorphology: A Comparative Review

Muchamad Ocky Bayu Nugroho¹

¹Universitas Pembangunan Nasional Veteran Yogyakarta, Faculty of Mineral Technology and Energy, Department of Geological Engineering, Sleman, Indonesia

Corresponding author: bayu.ocky@upnyk.ac.id

ABSTRACT

Submarine channels are major components that transport and store sediments across the continental margins that act as confined pathways for turbidity currents, facilitating sediment transfer from the shallow to the deep ocean and forming important sand-rich deposits with high hydrocarbon reservoir potential. Sedimentary processes are crucial for sculpting submarine channel morphologies and the building blocks of their architectural elements. This could be understood by seismic geomorphology analysis, which reveals the geological and geomorphological features through seismic data. Understanding the submarine channels through their morphology and architecture will help to build detailed geometry and evolution for further application, such as reservoir prediction, hydrocarbon migration and geological carbon storage. This review evaluates the effectiveness of seismic attributes in characterizing submarine channel geomorphology. This study examines 20 peer-reviewed articles published between 2016 and 2023 that applied seismic attribute analyses for geological interpretation of submarine channels. Seismic attributes such as RMS (root-mean square), variance, instantaneous frequency, sweetness, dip, curvature, coherence, and envelope were commonly applied in the reviewed case studies. Physical attributes highlight amplitude-related variations that may reflect lithological contrasts, depending on data calibration and depositional context, while geometrical attributes delineate channel margins and planform geometries and are strongly dependent on seismic data quality.

In cases where single attributes are insufficient to clearly reveal channel geomorphology, additional analyses such as co-rendering and spectral decomposition were employed to enhance interpretation. This study confirms that seismic attributes provide reliable insights into submarine channel deposits, including possible lithological contrasts, channel boundaries, channel-belt morphology, and the distribution of sediment accumulations within channel systems. However, the accuracy of interpretation depends on seismic data quality and the geological understanding of the study area. Inadequate knowledge or poor-quality seismic data can lead to misapplication of attribute parameters and potential misinterpretation.

Keywords: Seismic Interpretation, Seismic Attributes, Seismic Geomorphology, Submarine channels.

39 1. Introduction

40 Submarine channels are important morphological and sedimentary systems observed across
41 the continental slope to the deep. They facilitate sediment transport to the deep ocean by acting as
42 confined pathways for turbidity currents and serving as significant sand reservoirs with high
43 hydrocarbon potential (Pickering et al., 1989; Deptuck et al., 2007; Mulder et al., 2012;
44 Bouchakour et al., 2024 and 2025). These channels exhibit a dynamic response to variations in
45 seafloor topography (Posamentier and Kolla, 2003; Deb et al., 2012; Gamboa et al., 2012; Gamboa
46 & Alves, 2015; Bouchakour et al., 2022 and 2023). Over the past decade, submarine channels have
47 been widely studied due to the expansion of hydrocarbon exploration and the technological
48 evolution of data quality (Mayall et al., 2006, 2010; Weimer et al., 2007; Di Celma et al., 2010)
49 and their relevance in assessing geohazards (Bruschi et al., 2006; Thomas et al., 2010; Carter et
50 al., 2014). In addition, submarine channels can archive valuable sedimentological signatures and
51 paleoclimatic information that provide insights into the processes governing their formation
52 (Bouma, 2001; Brenchley et al., 2006; Zühlsdorff et al., 2007).

53 In many case studies, channel features are difficult to interpret properly due to poor seismic
54 data quality, limited seismic resolution, and pitfalls of time slice interpretation (Clark and
55 Pickering, 1996). The use of three-dimensional seismic data for interpretation of channel
56 geomorphology is referred to as seismic geomorphology (Posamentier et al., 2023). Seismic
57 geomorphology plays a key role in identifying and mapping the distribution of seismic facies
58 (Posamentier and Kolla, 2003; Posamentier, 2005). Seismic characteristics are obtained from
59 seismic data parameters and measurements such as amplitude, frequency, and attenuation, as well
60 as combinations of seismic attributes (Sheriff, 1994; Coren et al., 2001; Chopra and Marfurt,
61 2007a). Various reflection properties, including amplitude, dip magnitude, dip azimuth, time/depth
62 structure, and curvature, can be analyzed to generate direct images of features relevant to
63 deposition and structural frameworks (Posamentier, 2004). Seismic attributes are useful both
64 quantitatively and qualitatively. Quantitative applications involve predicting physical properties
65 such as porosity or lithology (Leiphart & Hart, 2001; Sagan & Hart, 2006), while qualitative uses
66 focus on identifying stratigraphic and structural elements (Hart, 2008). Over the past decades,
67 advances in seismic data visualization techniques and increased calibration through well ties have
68 enabled seismic attributes to provide valuable insights into geological structures, lithology, and
69 stratigraphic channels (Taner, 2001; Chopra & Marfurt, 2007a; Azevedo & Pereira, 2009). Among
70 their applications, the most critical is the extraction of information from raw seismic data that may
71 not be immediately apparent (Anees, 2013). Although seismic attributes are widely used by both
72 academic and industrial communities for geological and depositional interpretations, a number of
73 uncertainties remain when applying different attributes across varying geological settings and
74 datasets. Therefore, improving our understanding of seismic attribute behavior and systematically
75 testing their usefulness is essential.

76 This review aims to comprehensively evaluate the application of various seismic attributes in
77 interpreting channel system deposits within a seismic geomorphology framework. By synthesizing
78 case studies from the Taranaki Basin, Gulf of Mexico, Gulf of Thailand, Levant Basin, Offshore
79 Nile Delta, and Kribi-Campo Basin, this review highlights the specific roles, advantages, and

80 limitations of each attribute type in resolving channel morphology and associated depositional
81 features. The analysis also seeks to identify the most effective attributes for enhancing the
82 detection, visualization, and characterization of submarine channels, thereby providing guidance
83 for future exploration and geomorphological studies.
84

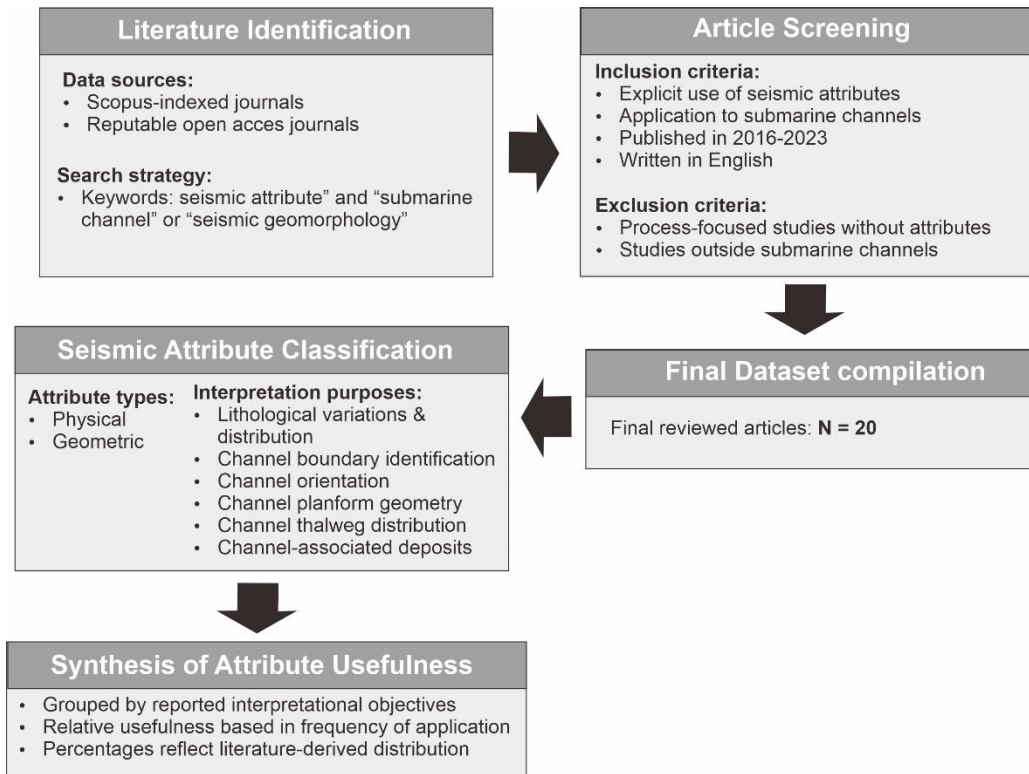
85 **2. Material and Methods**

86 This review was conducted using literature sourced from the Scopus database and reputable
87 open-access journals. The literature search applied targeted keywords, including “seismic
88 attribute” and “submarine channel” or “seismic geomorphology”, to prioritize studies explicitly
89 addressing seismic-based attribute analysis within a seismic geomorphology framework, while
90 maintaining a focused and reproducible review scope. This approach does not aim to provide an
91 exhaustive compilation of all related studies, and additional relevant literature may exist beyond
92 the selected keyword combinations. The keyword selection was designed to prioritize specificity
93 over completeness; consequently, studies addressing geological processes without explicit seismic
94 attribute analysis may not be fully represented. The inclusion criteria were as follows: (1) the
95 article was written in English, (2) it was published between 2016 and 2023, and (3) it explicitly
96 focused on seismic attributes and their application to submarine channel interpretation. The initial
97 search retrieved 28 articles from the Scopus database and one additional article from an open-
98 access journal. The selection of articles have been further optimized based on filtering works
99 focusing on submarine channel interpretation and their sedimentological context using 3D seismic
100 data. Following this process, a total of 20 articles were selected for this review. The scope of this
101 review focuses on the utilization of seismic attributes for interpreting submarine channel deposits
102 within a seismic geomorphology framework. The analysis addresses three main objectives: (1)
103 identifying the types of seismic attributes used, (2) classifying the attributes according to their
104 purposes in submarine channel characterization, and (3) evaluating their relative usefulness and
105 applicability for specific geomorphological and depositional objectives.

106 In this review, “usefulness” is defined in relation to the interpretation objectives established in
107 this study, rather than the original objectives of the individual case studies. It refers to the capability
108 of a seismic attribute to identify geological features based on a set of predefined interpretation
109 purposes established in this study, as evidenced by their application in the published literature. The
110 usefulness of each seismic attribute was evaluated using a qualitative binary scoring approach
111 based on six predefined interpretation purposes including lithological variation and distribution,
112 channel boundary identification, channel orientation, channel planform geometry, channel thalweg
113 distribution, and channel-associated deposits. Channel-associated deposits include channel-fill
114 sediments, levee–overbank deposits, and adjacent lobe or crevasse-splay deposits, which may be
115 expressed in seismic attribute maps through variations in amplitude, continuity, and geometric
116 patterns. For each attribute–purpose combination, a binary score of 1 was assigned when the
117 applicability of the attribute to a given purpose was explicitly demonstrated or could be reasonably
118 inferred from the interpretation results and discussion presented in the literature; otherwise, a score
119 of 0 was assigned. The usefulness score was calculated as the sum of achieved purposes divided

120 by the total number of purposes (six) and expressed as a percentage (%). The workflow of the
 121 review process is illustrated in Figure 1.

122
 123



124
 125
 126
 127
 128

Figure 1. Integrated workflow illustrating literature identification, screening, chronological selection, classification, and synthesis of seismic attribute applications in submarine channel studies

129 3. Results

130 The selected studies in this review employed a range of seismic attributes to characterize
 131 submarine channels. These include amplitude- and frequency-related attributes (e.g., RMS,
 132 envelope, sweetness, instantaneous frequency) as well as attributes that emphasize reflector
 133 continuity and geometry (e.g., coherence, variance, dip, and curvature) (Taner, 2001; Posamentier,
 134 2004; Chopra and Marfurt, 2006; Chopra and Marfurt, 2007a; Subrahmanyan and Rao, 2008;
 135 Posamentier et al., 2022). In most studies, these attributes are not interpreted individually but are
 136 integrated to provide complementary insights into channel geomorphology, stratigraphic
 137 architecture, and associated lithological variability.

138

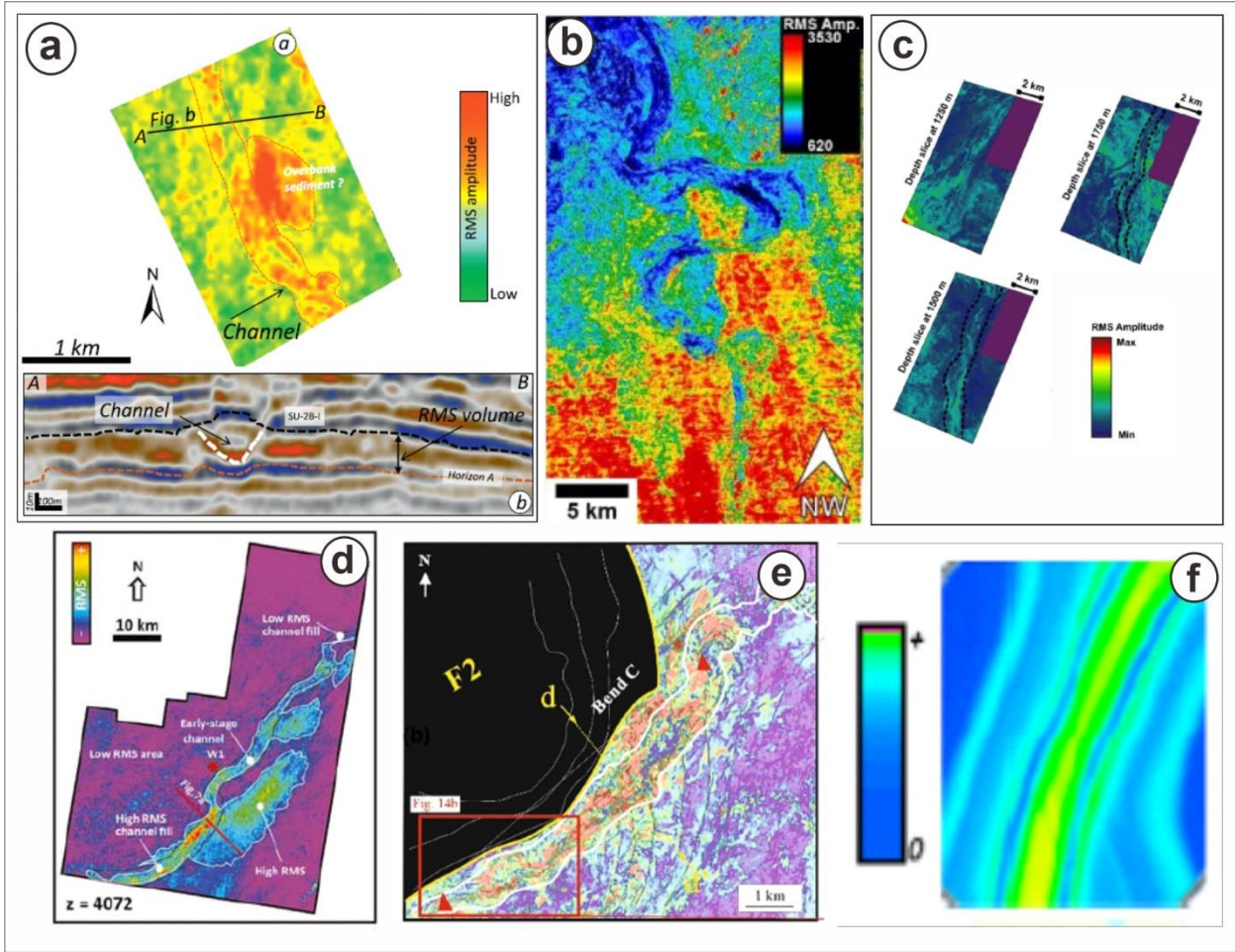
139 3.1. RMS Amplitude

140 RMS is calculated using the standard deviation, $\sigma(t)$, of the seismic amplitude values, $d(t)$,
 141 within a moving analysis window, where $\sigma(t)$ quantifies the dispersion of amplitude values around

142 their mean and thus provides a measure of reflectivity within that window (Taner, 2001; Chopra
143 and Marfurt, 2007a; Brown, 2004; Posamentier et al., 2022). The root-mean square (RMS)
144 attribute enhances high-amplitude reflections within specific intervals or horizons, thereby aiding
145 the delineation of channel-related depositional bodies and their planform geometries by
146 highlighting the lateral distribution and continuity of amplitude features (Brown, 2004; Omosanya
147 & Alves, 2013; Posamentier et al., 2022). It is calculated in specific time windows around horizons
148 where it reflects the signatures of reflection amplitudes and contrasts with background components
149 (Posamentier et al., 2022).

150 Figure 2a illustrates strong RMS attribute contrast within channel deposits. The channel is
151 expressed by relatively higher RMS amplitudes, suggesting a lithological contrast with the
152 surrounding lower-amplitude deposits, such as overbank or levee deposits. These are commonly
153 associated with coarser- and finer-grained lithologies, which should be confirmed by well data
154 calibration. The asymmetric distribution of high RMS amplitudes outside the channel margin
155 further suggests preferential sediment accumulation related to channel-adjacent depositional
156 processes, which may include overbank sedimentation and/or flow-stripping-related splay-like
157 deposits. The sinuous channel system is highlighted by elevated RMS amplitudes along the
158 channel thalweg and inner bends (Figure 2b). The high amplitude contrast suggests a different
159 lithological composition between the channel body and overbank deposits, potentially reflecting
160 sand-rich channel fills surrounded by fine-grained slope or overbank sediments. Localized
161 amplitude enhancement at channel bends is interpreted to reflect variations in seismic response
162 associated with changes in flow behavior along the curved channel pathway. Figure 2c illustrates
163 relatively high RMS amplitudes confined within the channel margins, indicating a contrast in
164 seismic response with the surrounding lower-amplitude channel-edge and overbank areas. The
165 integration with dip-angle attributes further assists in delineating channel edges and internal
166 stratigraphic boundaries associated with erosional surfaces. Figure 2d highlights along-channel
167 variations in RMS amplitude that reflect temporal changes in channel infill. The channels are
168 characterized by relatively high RMS amplitudes interpreted as sand-rich channel fills or possible
169 sediment splays. Figure 2e shows a pattern of relatively high RMS amplitude values that can be
170 interpreted as zones of preferential sand accumulation within the channel body. In contrast, Figure
171 2f shows a pronounced RMS amplitude contrast that clearly delineates channel boundaries,
172 reflecting a sensitivity analysis performed at a smaller scale on individual channel elements within
173 a channel complex (La Marca et al., 2023), where channel geometry and attribute responses can
174 be resolved more distinctly. Overall, these examples demonstrate that RMS amplitude is effective
175 for lithological variation, channel boundary identification, channel trend delineation, and the
176 interpretation of depositional elements within submarine channel deposits.

177
178

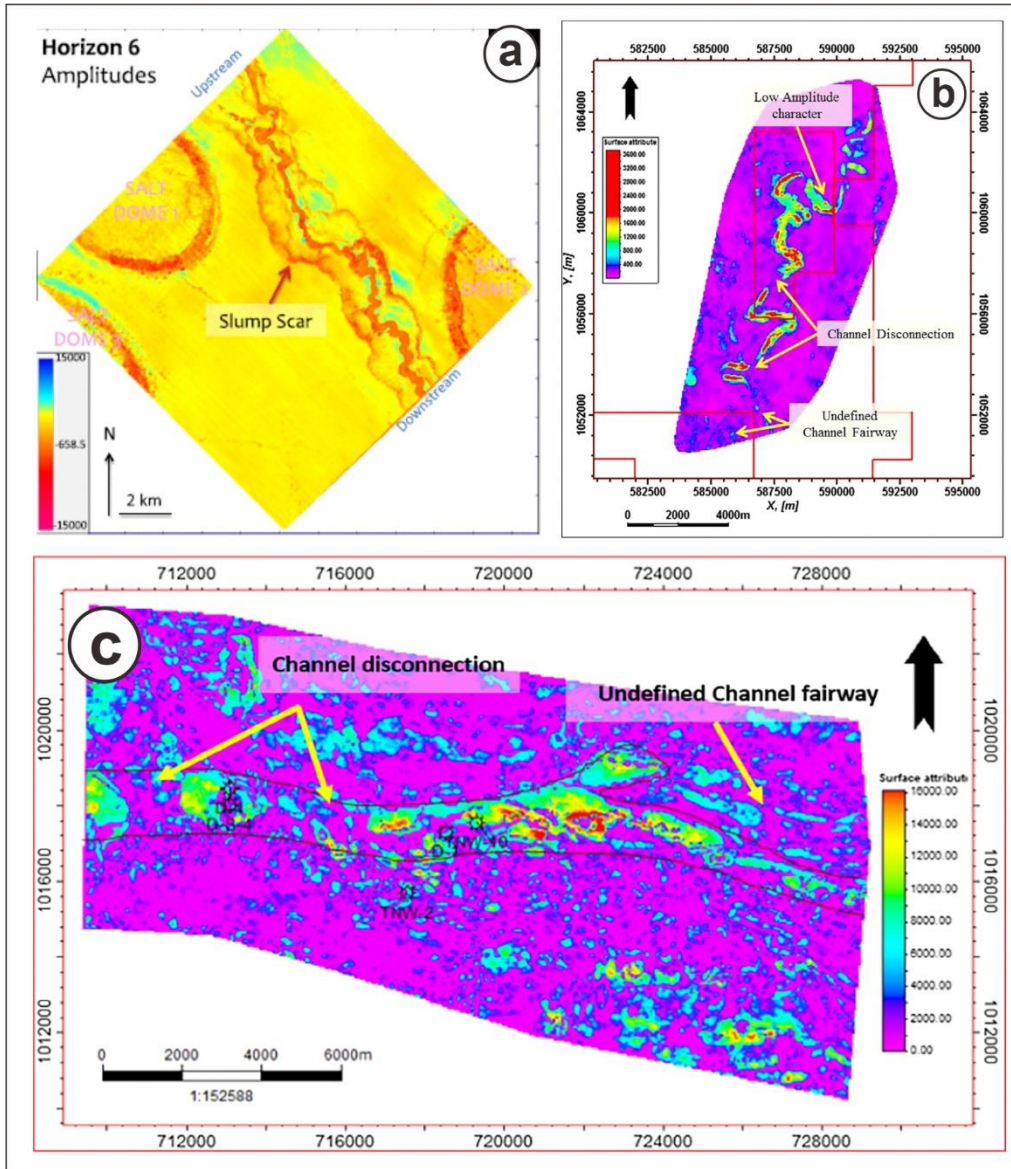


179
 180 Figure 2. Submarine channel geometries highlighted by the RMS amplitude attribute as reported in
 181 previous studies: (a) Levant Basin (Niyazi et al., 2018); (b) Taranaki Basin (Naewboonien, 2019); (c)
 182 Canterbury Basin (Harishidayat and Raja, 2022); (d) Kribi-Campo Basin (Gouott et al., 2023); (e) Niger
 183 Delta (Bouchakour et al., 2023); (f) Offshore New Zealand (La Marca et al., 2023)
 184

185 **3.2. Envelope Amplitude**

186 Envelope, also referred to as instantaneous amplitude, represents reflection strength
 187 independent of phase and highlights contrasts in acoustic impedance (Posamentier et al., 2022).
 188 Essentially, this attribute primarily captures variations in acoustic impedance, that may reflect
 189 subsurface reflectivity associated with lithological contrasts, internal stratigraphic heterogeneity,
 190 and variations in bed thickness (Subrahmanyam and Rao, 2008). The envelope is effective for
 191 emphasizing discontinuities, seismic facies variations, faults, depositional changes, tuning effects,
 192 sequence boundaries, and areas of hydrocarbon accumulation such as bright spots. As an
 193 amplitude-based attribute, envelope extractions reflect differences in density and velocity,
 194 facilitating high contrast in values corresponding to lithological changes and clearer delineation of
 195 the channel bodies. Figure 3a shows the envelope attribute extracted along the mapped horizon,
 196 exhibiting relatively low envelope values within portions of the channel body. It may reflect
 197 reduced reflection strength and locally disrupted seismic continuity within a defined amplitude

198 range. Such areas are interpreted to represent segments of the channel characterized by lower-
 199 amplitude seismic facies expression, associated with channel-related features such as channel
 200 margins and slump scars. In contrast, Figures 3b and 3c display envelope attributes extracted
 201 within a defined time window relative to the mapped horizon. These maps exhibit relatively high
 202 envelope values within the channel body, which are interpreted as sand-prone channel fills
 203 characterized by strong reflectivity. This interpretation is supported by calibration with well-log
 204 data, and the enhanced reflectivity facilitates the delineation of channel boundaries. The envelope
 205 also provides the amplitude context for other instantaneous attributes, particularly instantaneous
 206 frequency, which may become unstable in low-amplitude or noisy zones.
 207



208
 209 Figure 3. Submarine channel geometries highlighted by the envelope amplitude attribute as reported in
 210 previous studies: (a) Gulf of Mexico (Carter et al., 2016); (b) Nile Delta (Othman et al., 2016); (c) Nile
 211 Delta (Othman et al., 2018).

212
213
214
215
216
217
218
219
220
221
222
223
224
225
226
227
228
229
230
231
232
233
234
235
236
237
238
239
240
241
242
243
244
245
246

3.3. Instantaneous Frequency

Instantaneous frequency is computed as the time derivative of the instantaneous phase (Taner et al. 1979; Barnes 1991). The analytic signal also yields instantaneous amplitude (envelope), which is used to provide amplitude context for frequency interpretation. Subrahmanyam and Rao (2008) suggested that the instantaneous frequency attribute might reflect seismic-scale layer thickness and provide lithological insights. In some cases, it could be used to identify the thin-bed tuning effects and zones of abnormal seismic attenuation, where high-frequency energy is preferentially lost due to intrinsic absorption or scattering effects (Chopra and Marfurt, 2007a). Intrinsic absorption refers to energy loss caused by inelastic attenuation related to lithology, pore fluids, and rock properties, whereas scattering effects are triggered by small-scale heterogeneities such as thin interbedded sand–mud layers, erosional surfaces, or internal channel-fill complexity that redistribute seismic energy. Frequency-based seismic attributes are sensitive to seismic noise, and their application in stratigraphic and reservoir analysis remains limited in the industry. However, some studies have demonstrated their potential utility as part of an integrated attribute approach for identifying hydrocarbon-related indicators (Brown, 2011). As a physical attribute, the instantaneous frequency attribute has been shown to enhance the submarine channel features, including lithology prediction, depositional elements, and vertical layer thickness.

Figure 4a displays a channel pathway that is expressed by systematic variations in instantaneous frequency values relative to the surrounding background. The channel body is associated with contrasting frequency magnitudes, forming a continuous, sinuous pattern, while adjacent areas exhibit more uniform and laterally continuous frequency values. Figure 4b highlights that relatively lower instantaneous frequency values occur within the channel body and display pronounced spatial variability. The instantaneous frequency attribute enhances internal variability within the channel body, which may be associated with thin-bedded successions and internal heterogeneities linked to lateral channel migration and stacking patterns, rather than primary channel boundaries. The channel margins are more clearly delineated by sharp contrasts between higher and lower instantaneous frequency values, indicating that frequency magnitude variations enhance the visibility of channel geometry (Figure 4c). In vertical section, the channel interval is characterized by higher and laterally variable frequency values compared to the surrounding background strata which display lower and more uniform responses, with localized low-frequency anomalies potentially indicating attenuation or stratigraphic complexity within the channel fill (Figure 4d).

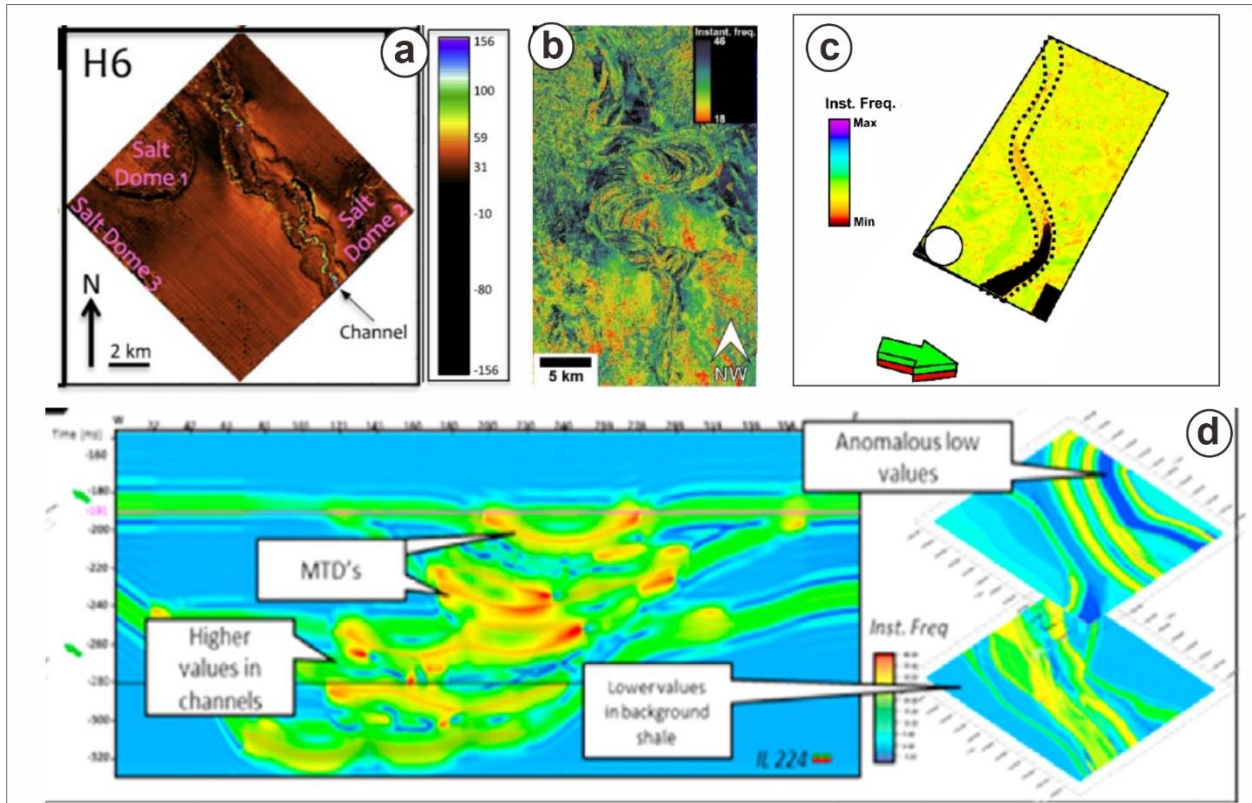


Figure 4. Submarine channel geometries highlighted by the instantaneous frequency attribute as reported in previous studies: (a) Gulf of Mexico (Carter et al., 2016); (b) Taranaki Basin (Naewboonien, 2019); (c) Canterbury Basin (Harishidayat and Raja, 2022); (d) Offshore New Zealand (La Marca et al., 2023).

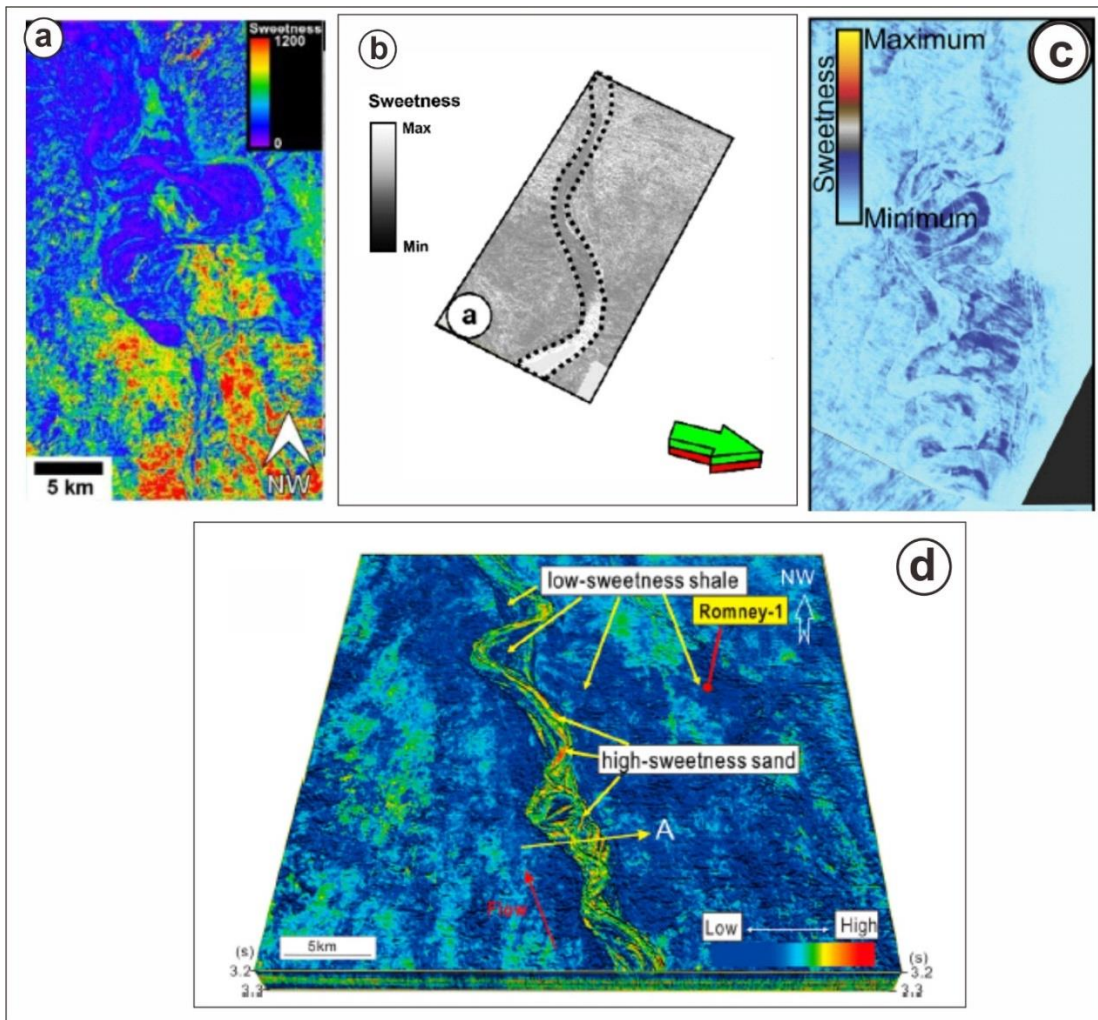
3.4. Sweetness

Sweetness is a composite seismic attribute designed to emphasize high-amplitude, low-frequency responses commonly associated with thick, clean reservoir-prone intervals. It is computed by dividing the instantaneous amplitude (or amplitude envelope) by the square root of the instantaneous frequency (Radovich and Oliveros, 1998). This attribute could be used for sand-shale ratio prediction. However, it is not particularly useful when the contrast in acoustic impedance between these lithologies is low (Hart, 2008). Theoretically, identifying the sand and shale composition that forms some trend or channel features is a means to illustrate the channel features more easily. On the other hand, several authors combine the sweetness attribute with geometrical attributes (coherence) to identify submarine channels in more detail (Li et al., 2017). The sweetness attribute becomes more effective for indicating potential pay zones when integrated with other seismic attributes, such as RMS amplitude, frequency, and phase, as demonstrated by Azeem et al. (2016) in the Sawan gas field, Pakistan. Figure 5a shows a plan-view sweetness attribute map in which the submarine channel body is characterized by relatively low to moderate sweetness values, consistent with a heterogeneous seismic response commonly associated with internally complex channel fills. In contrast, relatively higher sweetness values outside the channel

268 zone correspond to a more uniform seismic character which may be associated with a more
 269 homogeneous lithological composition.

270 In Figure 5b, the alignment between the interpreted channel margins (dashed lines) and the
 271 sweetness contrast demonstrates that sweetness is a robust attribute for channel boundary
 272 delineation, particularly in areas where amplitude alone may be ambiguous due to noise or tuning
 273 effects. Figure 5c highlights internal variations in sweetness within the channel belt, suggesting
 274 heterogeneity within the channel fill, potentially related to changes in grain size, layer thickness,
 275 or stacking patterns of channel elements. Figure 5d illustrates a sweetness attribute extracted along
 276 a time-slice horizon intersecting the submarine channel and integrated with well data, seismic
 277 inversion, and AVO analysis. Relatively high-sweetness anomalies along the channel axis are
 278 interpreted as sand-prone channel fills, supported by the association of strong amplitudes and
 279 reduced frequencies. In contrast, low-sweetness regions away from the channel axis are interpreted
 280 as shale-dominated background deposits.

281



282
 283 Figure 5. Submarine channel geometries highlighted by the sweetness attribute as reported in previous
 284 studies: (a) Taranaki Basin (Naewboonien, 2019); (b) Canterbury Basin (Harishidayat and Raja, 2022);
 285 (c) Taranaki Basin (Larsen et al., 2023); (d) Taranaki Basin (Li et al., 2017).

286 3.5. Variance and Coherence

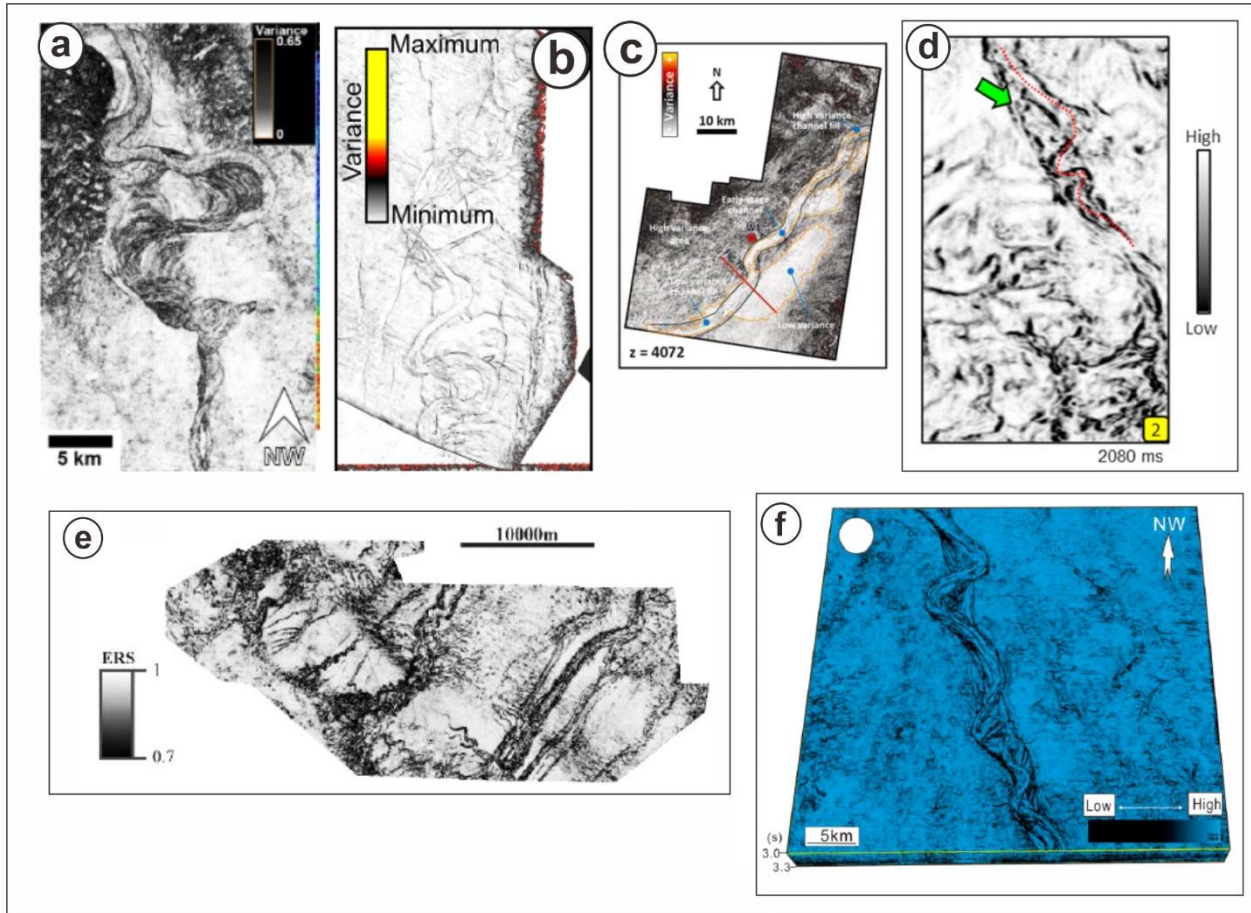
287 Variance and coherence are closely related seismic attributes that image lateral variations in
288 seismic signals over horizons or intervals and are widely used to enhance structural and
289 stratigraphic discontinuities (Posamentier et al., 2022). They are fundamental to seismic
290 interpretation and are commonly integrated with other attributes, such as RMS or RGB spectral
291 decomposition, to improve the visualization of channel architectures and associated features,
292 including mass-transport deposits (Almasgari et al., 2020; Howlett et al., 2022; Larsen et al.,
293 2023).. They are computed from trace-to-trace waveform similarity and statistical variability,
294 whereby seismic traces across faults or stratigraphic discontinuities exhibit reduced similarity
295 relative to surrounding, laterally continuous reflections (Bahorich and Farmer, 1995; Gersztenkorn
296 and Marfurt, 1999). The primary distinction between the two attributes lies in their computational
297 approach, where coherence relies on trace-to-trace similarity measures, whereas variance
298 quantifies statistical dispersion within a defined analysis window. Variance quantifies local
299 dissimilarities in seismic signals, while coherence evaluates the degree of similarity between
300 neighboring seismic traces (Posamentier et al., 2022). Together, coherence and variance enhance
301 the detection and visualization of seismic reflector discontinuities associated with faults and
302 stratigraphic changes, delineating fault planes and channel margins across both horizon slices and
303 vertical seismic sections.

304 These attributes are processed within a three-dimensional analysis window, this attribute
305 quantifies trace-to-trace variability across a sample interval, enhancing lateral acoustic impedance
306 contrasts associated with stratigraphic discontinuities such as channel belts and mass transport
307 complex as demonstrated by Bouchakour et al. (2022). Higher variance values correspond to zones
308 of increased discontinuity, for example where strong contrasts occur between the submarine
309 channel belt axis and its bounding levees (Naewbonieen, 2019). In contrast, coherence typically
310 exhibits low values along faults and stratigraphic boundaries, indicating geological discontinuities
311 associated with lateral changes in seismic character (Li et al., 2017). In terms of submarine channel
312 identification, coherence provides better constraints in distinguishing the channel axis from the
313 surrounding levee background compared to variance, as it is based on the similarity of seismic
314 traces. Similarity-based coherence evaluates a short “mini-trace” in multiple directions, allowing
315 systematic comparison with neighboring traces, which enhances sensitivity to subtle lateral
316 changes in seismic character and typically results in more precise delineation of channel-related
317 discontinuities (Posamentier et al., 2022).

318 Previous studies demonstrate that variance and coherence attributes enhance the imaging of
319 submarine channel architecture and are commonly used in combination with other seismic
320 attributes to improve channel delineation (Deptuck et al., 2007; Hansen et al., 2017; Li et al., 2017;
321 Naewboonien, 2019; Gouott et al., 2023; Larsen et al., 2023; La Marca et al., 2023; Silver and
322 Bedle, 2021; Bouchakour et al., 2025). Figure 6a shows that the variance attribute highlights high
323 trace-to-trace variability along sinuous channel margins, delineating erosional boundaries and
324 stepwise lateral channel shifting relative to the surrounding overbank deposits. Elevated variance
325 values delineate channel edges and zones of internal architectural complexity, reflecting abrupt

326 lateral changes in seismic character associated with channel incision and fill (Figure 6b). Figure
 327 6c exhibits low variance values outlining the channel axis, with additional associated channel-
 328 related elements, whereas higher variance values may indicate internal variability within the
 329 channel fill. The coherence attribute exhibits pronounced low-coherence lineaments along channel
 330 margins, clearly defining channel boundaries and zones of lateral discontinuity within the
 331 submarine channel system as shown in Figure 6d and 6e. Figure 6f further demonstrates that
 332 coherence contrasts effectively image channel margins and erosional features, enabling detailed
 333 mapping of channel geometry.

334
 335



336
 337 Figure 6. Examples of submarine channel identification using discontinuity-based seismic attributes as
 338 reported in previous studies: (a) variance attribute, Taranaki Basin (Naewboonien, 2019); (b) variance
 339 attribute, Taranaki Basin (Larsen et al., 2023); (c) variance attribute, Karibi/Campo Basin (Gouott et al.,
 340 2023); (d) coherence attribute, Offshore New Zealand (La Marca et al., 2023); (e) coherence attribute
 341 (ERS is energy ratio similarity), Taranaki Basin (Silver and Bedle, 2021); (f) coherence attribute,
 342 Taranaki Basin (Li et al., 2017)

343
 344
 345

346 **3.6. Dip Attribute**

347 The strike and dip of sedimentary layers are analogous to the magnitude and azimuth of the
348 dip. Marfurt (2006) emphasizes that accurate estimation of reflector dip magnitude and azimuth
349 (i.e., vector dip) constitutes the fundamental building block for geometric seismic attributes and
350 structurally oriented filtering. Such estimates can be obtained using several approaches, including
351 complex trace analysis, discrete vector dip scanning, and gradient structure tensor methods;
352 reliable vector dip estimation further enables the calculation of coherent amplitude gradients along
353 structural dip, thereby enhancing the delineation of subtle stratigraphic features such as channels
354 expressed through lateral variations in thin-bed tuning. Compared to variance and RMS attributes,
355 which primarily emphasize discontinuities and amplitude contrasts, dip attributes capture changes
356 in reflector orientation, providing improved imaging of subtle structural features surrounding or
357 crosscutting submarine channels, such as internal channel terraces. Dip magnitude represents the
358 magnitude of the reflector's local slope, quantifying the steepness of the seismic reflector relative
359 to the horizontal plane, with values ranging from 0 to 90. Dip azimuth defines the horizontal
360 direction of the maximum reflector slope and corresponds to the azimuthal direction of the vector
361 dip, typically measured clockwise from north or relative to the survey coordinate system. In terms
362 of submarine channel characterization, dip attributes reveal increased reflector tilting along
363 channel flanks, as well as a broad downstream gradient following the channel flow.

364 In recent quantitative workflows for submarine channel analysis, spatial variations in dip
365 magnitude have been used to highlight structural gradients and localized deformation, aiding the
366 identification of channel-bounding structural markers such as channel margins and bank failure-
367 related features (Bouchakour et al., 2025). Figure 7a exhibits systematic variations between low
368 and high dip azimuth values that define the sinuous channel pathway, including meandering
369 segments and shifts in channel orientation. These azimuthal contrasts emphasize channel curvature
370 and inferred flow direction, while also revealing the influence of adjacent salt domes that locally
371 deflect channel trajectories. The dip magnitude attribute shows higher dip angle values
372 concentrated along the channel flanks, reflecting increased reflector tilting associated with channel
373 incision and lateral relief, whereas lower dip magnitudes characterize the channel axis and produce
374 a clear and continuous expression of the channel thalweg (Figure 7b).

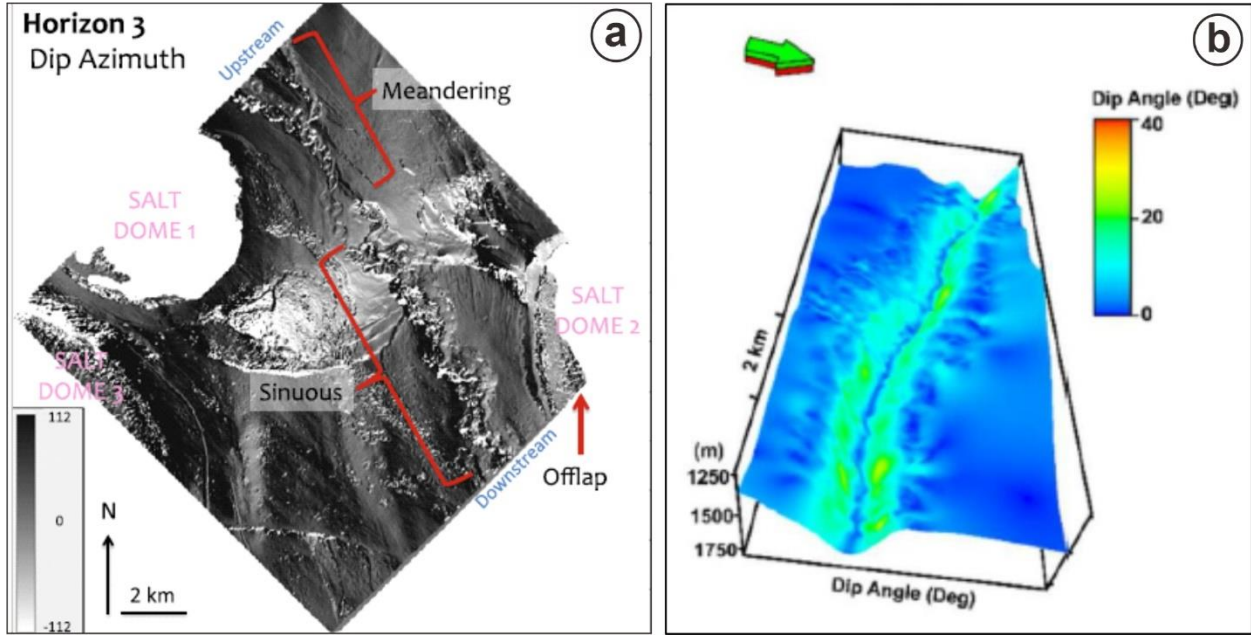


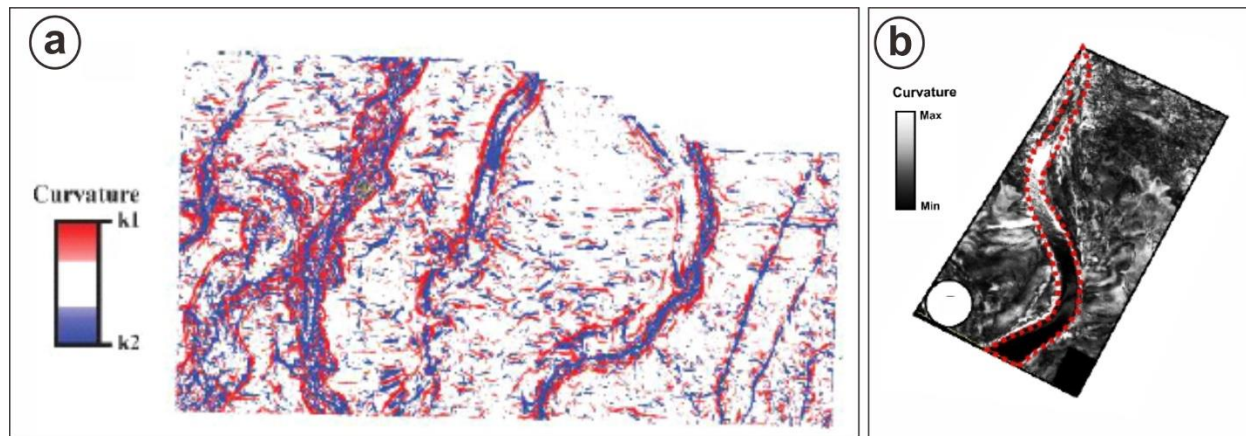
Figure 7. Dip attribute extraction identify submarine channel based on several authors (a) Gulf of Mexico (Carter et al., 2016); (b) Canterbury Basin (Harishidayat and Raja, 2022).

3.7. Curvature

Curvature is a three-dimensional seismic attribute that represents the local second-order geometric variation of a surface, quantifying the degree to which a horizon deviates from planarity (Chopra and Marfurt, 2006; Chopra and Marfurt, 2007b). By minimizing the influence of regional dip, curvature analysis enhances subtle, small-scale surface irregularities that are commonly associated with primary depositional elements or minor structural features such as small-scale faults. However, curvature attributes are sensitive to disrupted seismic images or limited depositional continuity, where noise, reflector truncation, or poor imaging may generate spurious curvature anomalies and lead to misleading geological interpretations. This attribute enhances subtle geometric irregularities and abrupt changes in surface curvature, making it particularly effective for identifying minor structural flexures and fault-related deformation.

Curvature can be applied to surfaces or time slices and is also helpful for the stratigraphic analysis of features such as channel margins, reefs, compaction structures, and debris flows (Chopra & Marfurt, 2007b). Two main types of curvature exist: (1) maximum curvature (k_{max}), defined as the curvature of a circle with the smallest radius and representing the direction of the most pronounced surface bending, and (2) minimum curvature (k_{min}), which characterizes the curvature of a second circle oriented perpendicular to the k_{max} direction and corresponds to the least pronounced bending of the surface at that point (Al-Dossary and Marfurt, 2006; Chopra and Marfurt, 2007b). In seismic geomorphology, maximum curvature commonly accentuates sharp ridges and levee crests, whereas minimum curvature emphasizes channel axes and erosional troughs, making the combined analysis particularly effective for delineating channel geometry and subtle structural deformation (Chopra and Marfurt, 2006; Chopra and Marfurt, 2007b). Positive values in the most-positive curvature (k_1) highlight concave-down structures, including channel banks and levees, while negative anomalies in the most-negative curvature (k_2) indicate concave-up features, such as the base of a channel (Figure 8a; Silver and Bedle, 2021). Figure 8b highlights

404 the contrast between minimum and maximum curvature which enhances the geometric definition
405 of the channel outline, allowing the channel pathway and boundaries to be accurately delineated.
406



407
408 Figure 8. Curvature attribute extraction identify submarine channel based on several authors (a) Taranaki
409 Basin (Silver and Bedle, 2021) (b) Canterbury Basin (Harishidayat and Raja, 2022).
410

411 4. Discussion

412 Since the 1990s, seismic attribute analysis has been increasingly applied to visualize and
413 interpret submarine channel deposits within deep-water systems, with continued methodological
414 development driven by advances in computerized seismic processing and interpretation
415 technologies (Posamentier and Kolla, 2003; Chopra and Marfurt, 2007; Mayall et al., 2010; Mayall
416 and Kneller, 2021; Bouchakour et al., 2022; Bouchakour et al., 2025). Many researchers have used
417 specific attributes and have made combinations between them or have applied additional methods
418 to enhance the visualization of channel features. For instance, spectral decomposition and RGB
419 color blending (Partyka et al., 1999; Chopra and Marfurt, 2007a; Carter et al., 2016; Othman et
420 al., 2018; Almasgari et al., 2020; Silver and Bedle, 2021; Bouchakour et al., 2023; Kamaruzaman
421 et al., 2023). Spectral decomposition has been widely integrated with other seismic attributes to
422 enhance the visualization of channel features by exploiting frequency-dependent seismic
423 responses, particularly in areas with limited seismic imaging quality or subtle channel expression.
424 This integration improves the identification of channel morphology and planform characteristics,
425 as well as associated depositional elements in submarine channel systems. Other studies have
426 applied co-rendering of two seismic attributes, typically integrating amplitude-based and
427 discontinuity-based attributes, to enhance the visualization of channel features (Li et al., 2017;
428 Niyazi et al., 2018; Naewboonien, 2019). Such integration provides effective visualization of
429 channel features but generally relies on good seismic image quality and clear channel expression.
430 Table 1 highlights a synthesis of the reviewed literature, illustrating how different seismic
431 attributes contribute to the identification of submarine channel deposits across various
432 interpretation purposes, as reflected by their respective usefulness scores. The review qualitatively
433 compares the effectiveness of seismic attributes in identifying channel features based on the
434 usefulness score.

435 The usefulness scores highlight clear contrasts between amplitude-based, frequency-related,
436 and geometric attributes in terms of their versatility and functional scope. Amplitude-related
437 attributes, particularly RMS amplitude, exhibit the highest usefulness score (100%), indicating that
438 they have been reported to support all predefined interpretation purposes. This reflects the well-
439 established sensitivity of RMS amplitude to changes in lithology and impedance contrasts, which
440 are fundamental to identifying channel boundaries, internal geometries, and associated
441 depositional elements (Posamentier and Kolla, 2003; Chopra and Marfurt, 2007a; Bernhardt et al.,
442 2012; Posamentier et al., 2022). The high applicability of RMS amplitude across studies
443 underscores its role as a first-order attribute in submarine channel analysis, particularly in settings
444 where sand–mud contrasts and stratigraphic variability are pronounced. Envelope amplitude and
445 sweetness attributes also show high usefulness scores (83.3%), suggesting broad applicability,
446 though dependent on geological and data quality context. This pattern indicates that amplitude-
447 derived attributes are highly effective for outlining channel architecture and depositional elements
448 but may be less consistently applied to more detailed geomorphological elements, depending on
449 data resolution and depositional complexity. Although instantaneous frequency can assist in
450 identifying lithological variations and channel-associated deposits, its application to channel trend
451 delineation and thalweg interpretation remains inconsistent, indicating strong context dependence.
452 This variability likely reflects the sensitivity of frequency attributes to tuning effects, attenuation,
453 and noise, which can complicate their application in laterally heterogeneous channel systems. The
454 high usefulness score of variance, coherence, and curvatures (83.3%) highlights their robustness
455 in capturing lateral discontinuities and channel margins, whereas the lower score of dip attributes
456 (66.7%) reflects their limited application in lithological prediction and channel-associated deposit
457 identification.

458 These results highlight that geometrical attributes are most effective when integrated with
459 physical attributes, underscoring the value of multi-attribute approaches in submarine channel
460 interpretation (Chopra and Marfurt, 2006; Chopra and Marfurt, 2007a; Chopra and Marfurt,
461 2007b). Overall, physical attributes provide lithological context, whereas geometrical attributes
462 define structural and morphological characteristics. Combining both types enhances overall
463 interpretation, and the usefulness score provides guidance on selecting the most suitable attributes
464 for specific geomorphological tasks. Attributes with lower usefulness scores should therefore not
465 be interpreted as having inferior performance; rather, they reflect a relative scarcity of documented
466 applications linking these attributes to specific interpretation purposes in the existing literature,
467 highlighting opportunities for further methodological exploration.

468
469
470
471
472
473
474
475

Table 1. The summary of seismic attribute application by interpretation purposes and their usefulness score

| No | Name of Attribute | Type of Attribute (Taner, 2001) | Interpretation purposes | Binary score | Usefulness score (%) |
|---------------------------------|-------------------------|---------------------------------|--|--------------------|--|
| 1 | RMS Amplitude | Physical | Lithological variations and distribution | 1 | 100 |
| | | | Channel boundary identification | 1 | |
| | | | Channel orientation | 1 | |
| | | | Channel planform geometry | 1 | |
| | | | Channel thalweg distribution | 1 | |
| | | | Channel-associated deposits | 1 | |
| | | | 2 | Envelope Amplitude | |
| Channel boundary identification | 1 | | | | |
| Channel orientation | 1 | | | | |
| Channel planform geometry | 1 | | | | |
| Channel thalweg distribution | 0 | | | | |
| Channel-associated deposits | 1 | | | | |
| 3 | Instantaneous Frequency | Physical | | | Lithological variations and distribution |
| | | | Channel boundary identification | 1 | |
| | | | Channel orientation | 0 | |
| | | | Channel planform geometry | 1 | |
| | | | Channel thalweg distribution | 0 | |
| | | | Channel-associated deposits | 1 | |
| | | | 4 | Sweetness | Physical |
| Channel boundary identification | 1 | | | | |
| Channel orientation | 1 | | | | |
| Channel planform geometry | 1 | | | | |
| Channel thalweg distribution | 0 | | | | |
| Channel-associated deposits | 1 | | | | |
| 5 | Variance & Coherence | Geometrical | | | |
| | | | Channel boundary identification | 1 | |
| | | | Channel orientation | 1 | |
| | | | Channel planform geometry | 1 | |
| | | | Channel thalweg distribution | 1 | |
| | | | Channel-associated deposits | 1 | |
| | | | 6 | Dip attribute | Geometrical |
| Channel boundary identification | 1 | | | | |

| | | | | | |
|---|-----------|-------------|--|---|------|
| | | | Channel orientation | 1 | |
| | | | Channel planform geometry | 1 | |
| | | | Channel thalweg distribution | 1 | |
| | | | Channel-associated deposits | 0 | |
| 7 | Curvature | Geometrical | Lithological variations and distribution | 0 | |
| | | | Channel boundary identification | 1 | |
| | | | Channel orientation | 1 | 83.3 |
| | | | Channel planform geometry | 1 | |
| | | | Channel thalweg distribution | 1 | |
| | | | Channel-associated deposits | 1 | |

478
479

480 **5. Conclusion**

481 This study investigated the usefulness of seismic attributes to visualize the morphologies of
 482 submarine channel systems and associated deposits within several areas, including Taranaki Basin,
 483 Gulf of Mexico, Gulf of Thailand, Levant Basin, Offshore Nile Delta, offshore Niger Delta, and
 484 Kribi-Campo Basin. The method used a qualitative review of 20 articles, which applied different
 485 techniques and attributes to their analysis. Generally, two types of seismic attributes were used
 486 according to Taner’s (2001) classification: physical attributes and geometrical attributes. Physical
 487 attributes include RMS amplitude, sweetness, envelope, and instantaneous frequency, whereas,
 488 geometrical attributes are variance, coherence, dip attribute, and curvature.

489 Physical attributes, particularly amplitude-based measures such as RMS amplitude, exhibit the
 490 broadest reported applicability across lithological, architectural, and depositional elements,
 491 highlighting their strong depositional usefulness in characterizing submarine channels and
 492 associated deposits. In contrast, geometrical attributes primarily enhance the delineation of channel
 493 boundaries, trends, and planform geometries, demonstrating pronounced morphological
 494 usefulness by capturing lateral discontinuities and channel-scale geometry rather than detailed
 495 lithological variations.

496 These results underscore that robust interpretation of submarine channel systems requires a
 497 purpose-driven integration of physical and geometrical attributes rather than reliance on any single
 498 attribute type. The direct application of individual seismic attributes may not always be sufficient
 499 and often requires complementary analyses such as attribute co-rendering, parameter tuning, and
 500 spectral decomposition. Overall, any interpretation method depends on seismic data quality and
 501 geological conditions. Therefore, strong geological understanding is essential in seismic
 502 interpretation and the use of the seismic attributes.

503
504
505

506 **6. References**

507

- 508 Al-Dossary, S., Marfurt, K.J. (2006). 3D volumetric multispectral estimates of reflector
509 curvature and rotation. *Geophysics* 71, P41–P51. <https://doi.org/10.1190/1.2242449>
- 510 Almasgari, A. A., Elsaadany, M., & Abdul Latiff, A. H. (2020). Application of seismic attributes
511 to delineate the geological features of the Malay Basin. *Bulletin of the Geological Society*
512 *of Malaysia*, 69, 97–110. <https://doi.org/10.7186/bgsm69202009>
- 513 Anees, M. (2013). Seismic attribute analysis for reservoir characterization. In *10th Biennial*
514 *International Conference and Exposition*. Society of Petroleum Geophysicists (SPG),
515 India, Paper P119.
- 516 Azeem, T., Yanchun, W., Khalid, P., Xueqing, L., Yuan, F., Lifang, C. (2016). An application of
517 seismic attributes analysis for mapping of gas bearing sand zones in the sawan gas field,
518 Pakistan. *Acta Geodaetica et Geophysica* 51, 723–744. [https://doi.org/10.1007/s40328-](https://doi.org/10.1007/s40328-015-0155-z)
519 [015-0155-z](https://doi.org/10.1007/s40328-015-0155-z)
- 520 Azevedo, L., & Pereira, G. R. (2009). Seismic attributes in hydrocarbon reservoir
521 characterization. Universidade de Aveiro, Departamento de Geociências.
- 522 Bahorich, M., & Farmer, S. (1995). 3D seismic discontinuity for faults and stratigraphic features:
523 The coherence cube. *The Leading Edge*, 14(10), 1053–1058.
524 <https://doi.org/10.1190/1.1437077>
- 525 Bernhardt, A., Stright, L., Lowe, D. R. (2012). Channelized debris-flow deposits and their
526 impact on turbidity currents: The Puchkirchen axial channel belt in the Austrian Molasse
527 Basin. *Sedimentology* 59, 2042–2070. <https://doi.org/10.1111/j.1365-3091.2012.01334.x>
- 528 Bouchakour, M., Zhao, X., Ge, J., Miclăuș, C., & Yang, B. (2022). Evolution of submarine
529 channel morphology in intra-slope mini-basins: 3D seismic interpretation from offshore
530 Niger Delta. *Marine and Petroleum Geology*, 146, 105912.
531 <https://doi.org/10.1016/j.marpetgeo.2022.105912>
- 532 Bouchakour, M., Zhao, X., Miclăuș, C., & Yang, B. (2023). Lateral migration and channel bend
533 morphology around growing folds (Niger Delta continental slope). *Basin Research*,
534 35(4), 1154–1192. <https://doi.org/10.1111/bre.12750>
- 535 Bouchakour, M., Zhao, X., Gamboa, D., Miclăuș, C., McArthur, A.D., Cao, S., Yang, L. (2025).
536 Kinematics of submarine channels in response to bank failures. *Basin Research* 37(1),
537 e70013. <https://doi.org/10.1111/bre.70013>
- 538 Bouma, A. H. (2001). Fine-grained submarine fans as possible recorders of long- and short-term
539 climatic changes. *Global and Planetary Change*, 28(1–4), 85–91
- 540 Brenchley, P. J., Marshall, J. D., & Harper, D. (2006). A late Ordovician (Hirnantian) karstic
541 surface in a submarine channel, recording glacio-eustatic sea-level changes: Meifod,
542 central Wales. *Geological Journal*, 41(1), 1–22. <https://doi.org/10.1002/gj.1039>

- 543 Brown, A. R. (2004). *Interpretation of three-dimensional seismic data*. American Association of
544 Petroleum Geologists and the Society of Exploration Geophysicists.
- 545 Brown, A. R. (2011). *Interpretation of three-dimensional seismic data (7th ed.)*. American
546 Association of Petroleum Geologists Memoir 42/ Society of Exploration Geophysicists
547 investigation in geophysics, no. 9. <https://doi.org/10.1306/m4271346>
- 548 Bruschi, R., Bughi, S., Spinazzè, M., Torselletti, E., & Vitali, L. (2006). Impact of debris flows
549 and turbidity currents on seafloor structures. *Norwegian Journal of Geology*, 86, 317–
550 337. https://njg.geologi.no/images/NJG_articles/60713_NGT_no_3_06_18.pdf
- 551 Carter, L., Gavey, R., Talling, P. J., & Liu, J. T. (2014). Insights into submarine geohazards from
552 breaks in subsea telecommunication cables. *Oceanography*, 27(2), 58–67.
553 <https://doi.org/10.5670/oceanog.2014.40>
- 554 Carter, C., Gani, M., Roesler, T., & Sarwar, A. (2016). Submarine channel evolution linked to
555 rising salt domes, Gulf of Mexico, USA. *Sedimentary Geology*, 342, 237–253.
556 <https://doi.org/10.1016/j.sedgeo.2016.06.021>
- 557 Chopra, S., Marfurt, K. (2006). Seismic Attributes – a promising aid for geologic prediction.
- 558 Chopra, S., & Marfurt, K. J. (2007a). Seismic attributes for prospect identification and reservoir
559 characterization (457 p.). *Society of Exploration Geophysicists*.
560 <https://doi.org/10.1190/1.9781560801900>
- 561 Chopra, S., Marfurt, K. (2007b). Curvature attribute applications to 3D surface seismic data. *The*
562 *Leading Edge* 26, 404–414. <https://doi.org/10.1190/1.2723201>
- 563 Clark, J. D., & Pickering, K. T. (1996). Architectural elements and growth patterns of submarine
564 channels: Application to hydrocarbon exploration. *AAPG Bulletin*, 80(2), 194–221.
565 <https://doi.org/10.1306/64ED8819-1724-11D7-8645000102C1865D>
- 566 Coren, F., Volpi, V., & Tinivella, U. (2001). Gas hydrate physical properties imaging by
567 multiattribute analysis—Blake Ridge BSR case history. *Marine Geology*, 178(1), 197–
568 210. [https://doi.org/10.1016/S0025-3227\(01\)00198-5](https://doi.org/10.1016/S0025-3227(01)00198-5)
- 569 Deb, M., Das, D., & Uddin, M. (2012). Evaluation of meandering characteristics using RS &
570 GIS of Manu River. *Journal of Water Resource and Protection*, 4(3), 163–171.
571 <https://doi.org/10.4236/jwarp.2012.43019>
- 572 Deptuck, M. E., Sylvester, Z., Pirmez, C., & O’Byrne, C. (2007). Migration–aggradation history
573 and 3-D seismic geomorphology of submarine channels in the Pleistocene Benin major
574 canyon, western Niger Delta slope. *Marine and Petroleum Geology*, 24(6–9), 406–433.
575 <https://doi.org/10.1016/j.marpetgeo.2007.01.005>
- 576 Di Celma, C., Cantalamessa, G., Didaskalou, P., & Lori, P. (2010). Sedimentology, architecture,
577 and sequence stratigraphy of coarse-grained, submarine canyon fills from the Pleistocene
578 (Gelasian–Calabrian) of the Peri-Adriatic Basin, central Italy. *Marine and Petroleum*
579 *Geology*, 27(6), 1340–1365. <https://doi.org/10.1016/j.marpetgeo.2010.05.011>

- 580 Gamboa, D., Alves, T. M., & Cartwright, J. (2012). A submarine channel confluence
581 classification for topographically confined slopes. *Marine and Petroleum Geology*, 35(1),
582 176–189. <https://doi.org/10.1016/j.marpetgeo.2012.02.011>
- 583 Gamboa, D., & Alves, T. M. (2015). Spatial and dimensional relationships of submarine slope
584 architectural elements: A seismic-scale analysis from the Espírito Santo Basin (SE
585 Brazil). *Marine and Petroleum Geology*, 64, 43–57.
586 <https://doi.org/10.1016/j.marpetgeo.2015.01.014>
- 587 Gersztenkorn, A., & Marfurt, K. J. (1999). Eigenstructure-based coherence computations as an
588 aid to 3D structural and stratigraphic mapping. *Geophysics*, 64(5), 1468–1479.
589 <https://doi.org/10.1190/1.1444651>
- 590 Gouott, B.S.B., Mbida Yem, Atangana, J.Q.Y., Nkoa, P.E.N., Biouele, S.E.A., Niyazi, Y., &
591 Eruteya, O.E. (2022). Seismic geomorphology of a Late Cretaceous submarine channel
592 system in the Kribi/Campo sub-basin, offshore Cameroon. *Marine and Petroleum*
593 *Geology*, 145, 105865. <https://doi.org/10.1016/j.marpetgeo.2022.105865>
- 594 Hansen, L., Janocko, M., Kane, I., Kneller, B. (2017). Submarine channel evolution, terrace
595 development, and preservation of intra-channel thin-bedded turbidites: Mahin and Avon
596 channels, offshore Nigeria. *Marine Geology* 383, 146–167.
597 <https://doi.org/10.1016/j.margeo.2016.11.011>
- 598 Hart, B. S. (2008). Channel detection in 3-D seismic data using sweetness. *AAPG Bulletin*, 92(6),
599 733–742. <https://doi.org/10.1306/02050807127>
- 600 Harishidayat, D., & Raja, W. R. (2022). Quantitative seismic geomorphology of four different
601 types of the continental slope channel complexes in the Canterbury Basin, New Zealand.
602 *Applied Sciences*, 12(9), 4386. <https://doi.org/10.3390/app12094386>
- 603 Howlett, D.M., Gawthorpe, R.L., Ge, Z., Rotevatn, A., Jackson, C.A.-L. (2021). Turbidites,
604 topography and tectonics: Evolution of submarine channel-lobe systems in the salt-
605 influenced Kwanza Basin, offshore Angola. *Basin Research* 33, 1076–1110.
606 <https://doi.org/10.1111/bre.12506>
- 607 Kamaruzaman, E. H., La Croix, A. D., & Kamp, P. J. J. (2023). Quantitative seismic
608 geomorphology of sediment conduits on an evolving Miocene slope in Taranaki Basin
609 (New Zealand): The influence of increasing slope gradient through time. *Marine and*
610 *Petroleum Geology*, 152, 106233. <https://doi.org/10.1016/j.marpetgeo.2023.106233>
- 611 La Marca, K., Bedle, H., Stright, L., & Marfurt, K. (2023). Sensitivity analysis of seismic
612 attributes parametrization to reduce misinterpretations: Applications to deepwater
613 channel complexes. *Marine and Petroleum Geology*, 153, 106309.
614 <https://doi.org/10.1016/j.marpetgeo.2023.106309>
- 615 Larsen, C., Harishidayat, D., & Omosanya, K. O. L. (2023). Geomorphologic control on the
616 evolution of Middle-Late Miocene submarine channels in the Southern Taranaki Basin,

- 617 New Zealand. *Marine and Petroleum Geology*, 156, 106447.
618 <https://doi.org/10.1016/j.marpetgeo.2023.106447>
- 619 Leiphart, D. J., & Hart, B. S. (2001). Comparison of linear regression and a probabilistic neural
620 network to predict porosity from 3-D seismic attributes in Lower Brushy Canyon
621 channelled sandstones, southeast New Mexico. *Geophysics*, 66(5), 1349–1358.
622 <https://doi.org/10.1190/1.1487080>
- 623 Li, Q., Yu, S., Wu, W., Tong, L., & Kang, H. (2017). Detection of a deep-water channel in 3D
624 seismic data using the sweetness attribute and seismic geomorphology: A case study from
625 the Taranaki Basin, New Zealand. *New Zealand Journal of Geology and Geophysics*,
626 60(2), 199–208. <https://doi.org/10.1080/00288306.2017.1307230>
- 627 Marfurt, K.J. (2006). Robust estimates of 3D reflector dip and azimuth. *Geophysics* 71, P29–
628 P40. <https://doi.org/10.1190/1.2213049>
- 629 Mayall, M., Jones, E., & Casey, M. (2006). Turbidite channel reservoirs—Key elements in facies
630 prediction and effective development. *Marine and Petroleum Geology*, 23(9), 821–841.
631 <https://doi.org/10.1016/j.marpetgeo.2006.08.001>
- 632 Mayall, M., Lonergan, L., Bowman, A., James, S., Mills, K., Primmer, T., Pope, D., Rogers, L.,
633 & Skeene, R. (2010). The response of turbidite slope channels to growth-induced seabed
634 topography. *AAPG Bulletin*, 94(7), 1011–1030. <https://doi.org/10.1306/01051009117>
- 635 Mayall, M., and Kneller, B. (2021). Seismic interpretation workflows for deep-water systems: A
636 practical guide for the subsurface. *Bulletin*, 105, 2127–2157.
637 <https://doi.org/10.1306/05262120094>
- 638 Mulder, T., Ducassou, H. E., Gillet, H., Hanquiez, V., Tournadour, E., Combes, J., Elberli, P.,
639 Kindler, P., Gonthier, E., & Gones, G. (2012). Canyon morphology on a modern
640 carbonate slope of the Bahamas: Evidence of regional tectonic tilting. *Geology*, 40(9),
641 771–774. <https://doi.org/10.1130/G33327.1>
- 642 Naewboonien, K. (2019). The use of seismic attributes for submarine channel interpretation in
643 deepwater Taranaki Basin, New Zealand. *Bulletin of Earth Science of Thailand*, 11, 134–
644 143. . <https://doi.org/10.14456/best.2019.15>
- 645 Niyazi, Y., Eruteya, O. E., Omosanya, K. O., Harishidayat, D., Johansen, S. E., & Waldmann, N.
646 (2018). Seismic geomorphology of submarine channel-belt complexes in the Pliocene of
647 the Levant Basin, offshore central Israel. *Marine Geology*, 403, 123–138.
648 <https://doi.org/10.1016/j.marpetgeo.2018.05.007>
- 649 Omosanya, K. O., & Alves, T. M. (2013). A 3-dimensional seismic method to assess the
650 provenance of mass-transport deposits (MTDs) on salt-rich continental slopes (Espírito
651 Santo Basin, SE Brazil). *Marine and Petroleum Geology*, 44, 223–239.
652 <http://dx.doi.org/10.1016/j.marpetgeo.2013.02.006>

- 653 Othman, A. A. A., Fathy, M., & Maher, A. (2016). Use of spectral decomposition technique for
654 delineation of channels at Solar gas discovery, offshore West Nile Delta, Egypt. *Egyptian*
655 *Journal of Petroleum*, 25(1), 45–51. <https://doi.org/10.1016/j.ejpe.2015.03.005>
- 656 Othman, A. A. A., Fathy, M., & Negm, A. (2018). Identification of channel geometries applying
657 seismic attributes and spectral decomposition techniques, Tamsah Field, Offshore East
658 Nile Delta, Egypt. *NRIAG Journal of Astronomy and Geophysics*, 7, 52–61.
659 <https://doi.org/10.1016/j.nrjag.2018.04.001>
- 660 Partyka, G., Gridley, J., & Lopez, J. (1999). Interpretational applications of spectral
661 decomposition in reservoir characterization. *The Leading Edge*, 18(3), 353–360.
662 <https://doi.org/10.1190/1.1438295>
- 663 Pickering, K. T., Hiscott, R. N., & Hein, F. J. (1989). *Deep marine environments*. Harper-Collins
664 (Chapman & Hall).
- 665 Posamentier, H. W., & Kolla, V. (2003). Seismic geomorphology and stratigraphy of
666 depositional elements in deep-water settings. *Journal of Sedimentary Research*, 73(3),
667 367–388. <https://doi.org/10.1306/111302730367>
- 668 Posamentier, H. W. (2004). Seismic geomorphology: Imaging elements of depositional systems
669 from shelf to deep basin using 3D seismic data: Implications for exploration and
670 development. In *3D seismic technology: Application to the exploration of sedimentary*
671 *basins* (Vol. 29, pp. 11–24). Geological Society, London, Memoirs.
672 <https://doi.org/10.1144/GSL.MEM.2004.029.01.0>
- 673 Posamentier, H. W. (2005). Application of 3D Seismic Visualization Techniques for Seismic
674 Stratigraphy, Seismic Geomorphology, and Depositional Systems Analysis: Examples
675 from Fluvial to Deep-Marine Depositional Environments. *Petroleum Geoscience* 6:
676 1565–1576. <https://doi.org/10.1144/0061565>
- 677 Posamentier, H. W., Paumard, V., & Lang, S. C. (2022). Principles of seismic stratigraphy and
678 seismic geomorphology I: Extracting geologic insights from seismic data. *Earth-Science*
679 *Reviews*, 228, 103963. <https://doi.org/10.1016/j.earscirev.2022.103963>
- 680 Sagan, J. A., & Hart, B. S. (2006). 3-D seismic and structural investigation of a hydrothermal
681 dolomite reservoir in the Trenton-Black River, Saybrook, Ohio. *AAPG Bulletin*, 90(11),
682 1763–1785. <https://doi.org/10.1306/07190605027>
- 683 Sheriff, R. E. (1994). *Encyclopedia dictionary of exploration geophysics*. Society of Exploration
684 Geophysicists. <https://doi.org/10.1190/1.9781560802969>
- 685 Silver, C., & Bedle, H. (2021). Evolution of a Late Miocene deep-water depositional system in
686 the Southern Taranaki Basin, New Zealand. *Geosciences*, 11(8), 329.
687 <https://doi.org/10.3390/geosciences11080329>
- 688 Subrahmanyam, P., & Rao, P. H. (2008). Seismic attributes – A review. In *7th International*
689 *Conference and Exposition on Petroleum Geophysics*. <https://spgindia.org/2008/398.pdf>

- 690 Taner, M. T. (2001). Seismic attributes. *Canadian Society of Exploration Geophysicists*
691 *Recorder*, September, 49–56.
- 692 Thomas, S., Hooper, J., & Clare, M. (2010). Constraining geohazards to the past: Impact
693 assessment of submarine mass movements on seabed developments. In *Submarine mass*
694 *movements and their consequences, Advances in Natural and Technological Hazards*
695 *Research* (pp. 387–398). Springer. https://doi.org/10.1007/978-90-481-3071-9_32
- 696 Weimer, P., Slatt, R. M., & Bouroullec, R. (2007). *Introduction to the petroleum geology of*
697 *deepwater settings*. AAPG/Datapages Tulsa. <https://doi.org/10.1306/St571314C16>
- 698 Zühlsdorff, C., Wien, K., Stuet, J.-B. W., & Henrich, R. (2007). Late Quaternary sedimentation
699 within a submarine channel–levee system offshore Cap Timiris, Mauritania. *Marine*
700 *Geology*, 240(1–4), 217–234. <https://doi.org/10.1016/j.margeo.2007.02.005>

701

702

703

704

705